Muon anomalous magnetic moment constraints on supersymmetric U(1)′ models

Elif Cincioğlu,[1] Zerrin Kırca,[1,2] Hale Sert,[3] Saime Solmaz,[1] Levent Solmaz,[1] and Yasar Hiçyılmaz[1]
[1]*Department of Physics, Balıkesir University, TR10145, Balıkesir, Turkey*
[2]*Department of Physics, Uludağ University, TR16000, Bursa, Turkey*
[3]*Department of Physics, İzmir Institute of Technology, TR35430, İzmir, Turkey*
(Received 24 June 2010; published 10 September 2010)

We study the anomalous magnetic moment of the muon in supersymmetric E_6 models and generic U(1)′ models to probe the model reactions and to find constraints on the large parameter space of these models. For future searches, by imposing the existing bounds coming from collider searches and theoretical considerations upon the U(1)′ model parameters, we examine the lightest Higgs boson mass m_h and the mass of the additional Z boson m_{Z_2} in such singlet extensions of the MSSM. We observed that not only supersymmetric E_6 models but also generic U(1)′ models are sensitive to the imposition of the considered bounds. Indeed, without the muon anomaly constraints E_6 models and generic U(1)′ models can predict m_h as large as ~150 GeV and ~180 GeV, respectively. However, in addition to the mentioned constraints when a 1σ range for the anomalous magnetic moment of the muon is considered, we observe that generic U(1)′ models do not favor the mass of the lightest Higgs boson to be larger than 140 GeV; it should be smaller than 135 GeV in E_6 models.

DOI: 10.1103/PhysRevD.82.055009 PACS numbers: 12.60.Cn, 13.40.Em, 14.80.Da

I. INTRODUCTION

Even if none of the particles predicted within the supersymmetric theories are detected yet, such extensions of the standard model (SM) are attractive new physics scenarios because they offer a number of plausible explanations for a number of issues ranging from dark matter candidates to the stabilization of the Higgs mass. But the most popular and economical model, the minimal supersymmetric standard model (MSSM) [1], suffers from the μ problem [2], solution of which demands certain extensions among which singlet extended supersymmetric models, such as U(1)′ models, occupy a special place [3].

Another motivation for considering supersymmetric models comes from the observed anomaly in the magnetic moment measurements of the muon. Indeed, there is a difference between experimental determination of the muon magnetic moment and theoretical prediction calculated according to the SM. This difference may stem from hadronic uncertainties in the SM calculations and/or it stems from new physics. We will, based on the latter possibility, use this difference to find constraints on the U(1)′ models.

On the experimental side, a series of precision measurements of the muon anomalous magnetic moment, $a_\mu = (g-2)/2$, at Brookhaven National Laboratory E821 experiment [4] improved the previous measurements at CERN and enabled one to deduce

$$a_\mu^{\mathrm{Exp}} = (11\,659\,208 \pm 6) \times 10^{-10}. \quad (1)$$

This value was, very recently, updated to be [5]

$$a_\mu^{\mathrm{Exp}} = (116\,592\,089 \pm 63) \times 10^{-11}. \quad (2)$$

On the theoretical side, and according to the SM, the predicted value of a_μ is somewhat smaller than the experimental result:

$$a_\mu^{\mathrm{SM}} = (116\,591\,773 \pm 48) \times 10^{-11}, \quad (3)$$

which shows approximately 3–4σ difference [5]. In the SM a_μ prediction consists of three parts: QED, electroweak, and hadronic contribution among which the latter dominates the theoretical uncertainty [6]. Indeed, hadronic leading-order contributions based on e^+e^- and τ data differ. If τ-based data are used instead e^+e^- ones then the discrepancy drops to 1–2σ [7,8]. In this work we prefer to use e^+e^- data in order to find constraints on the U(1)′ models. But if one uses the τ-based data rather than the e^+e^- data for the hadronic leading-order contributions to the anomalous magnetic moment of the muon, then the allowed region shifts substantially and our results would change.

Briefly, standard deviation of the muon magnetic moment between SM prediction and experimental value is non-negligible and the following value may be an indication of new physics [5]:

$$\delta a_\mu = a_\mu^{\mathrm{Exp}} - a_\mu^{\mathrm{SM}} = (316 \pm 79) \times 10^{-11}. \quad (4)$$

As a matter of fact, the present anomaly has resulted in a variety of supersymmetric explanations, including the minimal model [9]. Additionally, the next-to-minimal supersymmetric standard model (NMSSM) [10] and U(1)′ explanations dealing with the same issue exist in the literature [11]. Beyond that, the anomalous magnetic moment of the muon can be used to find constraints on extended model parameters and hence this anomaly can be used to make educated guesses for supersymmetric models.

Hence, in this work, we will study its impact on the generic and E_6-based supersymmetric U(1)′ models. By using the mentioned anomaly we will constrain the parameter space of generic and E_6-based U(1)′ models. Additionally, by using the constrained parameter space, we will make predictions for the lightest Higgs mass m_h and the additional Z mass m_{Z_2} which can be illuminating for future measurements.

The organization of the present study is as follows. In the following section we introduce salient features of the U(1)′ models stemming from E_6 grand unified theory (GUT) and generic models. In the same section we will overview different contributions to the magnetic moment of the muon within U(1)′ models as subsections. In Sec. III we present our numerical results. And we conclude in Sec. IV.

II. SALIENT FEATURES OF THE U(1)′ MODEL

There are bottom-up and top-down reasons for considering U(1)′ models. From bottom-up, to begin with, the U(1)′ model can generate the neutrino masses in the correct experimental range via Dirac type coupling. In addition to the ordinary Higgs fields of the MSSM, an additional scalar field S exists in the U(1)′ model and this field is responsible for generating the μ parameter around the weak scale. Furthermore, a viable cold dark matter candidate exists within the U(1)′ model for a reasonable set of parameters [12]. Another attractive aspect is that in U(1)′ models the lightest Higgs boson weighs significantly more than M_Z even without loop corrections [13]. Besides this, the U(1)′ models can explain a number of phenomena ranging from LEP indications for two light Higgs bosons [14] to the recent Tevatron Higgs mass measurements [15] (see references therein).

From top-down, U(1)′ models typically arise from supersymmetric grand unified theories and superstrings [16]. From E_6 GUT, for instance, two extra U(1) symmetries appear in the breaking $E_6 \rightarrow SO(10) \times \mathrm{U}(1)_\psi$ followed by $SO(10) \rightarrow SU(5) \times \mathrm{U}(1)_\chi$ where $\mathrm{U}(1)_{Y'}$ is a linear combination of ψ and χ symmetries. In this picture, Ψ and χ are the basic models (charge assignments of the models can be read from Table I) of the U(1)′ model and the resulting model consists of a linear combination of these two different models which is designated by a mixing angle $\theta_{E(6)}$ varying from 0 to π:

TABLE I. U(1)′ charges in χ and ψ models, taken from [16].

	$2\sqrt{10}Q_\chi$	$2\sqrt{6}Q_\psi$
u, d, u^c, e^+	−1	1
d^c, ν, e^-	3	1
ν^c	−5	1
H_u	2	−2
H_d	−2	−2
S	0	4

$$Q(\theta_{E_6}) = \cos\theta_{E_6} Q_\chi + \sin\theta_{E_6} Q_\psi + \xi. \tag{5}$$

In the above equation (5), ξ refers to kinetic mixing since there are more than one U(1) factor, but we will omit this term for simplicity. Meanwhile, by varying the value of mixing angle θ_{E_6} in the $(0,\pi)$ range there arises, in fact, a continuum of E_6-based U(1)′ models [17] which can absorb small ξ values.

Besides the authentic E_6 models, different U(1)′ models exist in the literature in which charge assignments and particle content differ from the original setups (for instance, see [18,19]). We aim to study generic U(1)′ models in addition to the original ones. But in generic U(1)′ models one faces certain problems such as triangular anomalies and hence gauge coupling nonunification. Whereas, in the E_6 models, by construction, all anomalies are canceled out when the complete E_6 multiplets are included [20]. For a generic U(1)′, with minimal matter spectrum, cancellation is nontrivial. One option is to introduce U(1)′ models with family-dependent charges [18]. Another option in this direction is that anomalies are canceled by heavy states (beyond the reach of the LHC) weighing near the TeV scale or more. We will follow this possibility.

Effectively, our U(1)′ models—generic or E_6 based—are characterized by the gauge structure

$$SU(3)_C \times SU(2)_L \times \mathrm{U}(1) \times \mathrm{U}(1)', \tag{6}$$

for which g_3, g_2, g_1, and g'_Y are the corresponding gauge couplings. The following superpotential

$$\hat{W} = h_u \hat{Q} \cdot \hat{H}_u \hat{U}^c + h_d \hat{Q} \cdot \hat{H}_d \hat{D}^c + h_e \hat{L} \cdot \hat{H}_d \hat{E}^c + h_s \hat{S} \hat{H}_u \cdot \hat{H}_d \tag{7}$$

parametrizes U(1)′ models of interest where we discarded additional fields. In generic models we will use U(1)′ gauge invariance to find constraints on the U(1)′ charges.

The soft breaking terms, with the most general holomorphic structures, are

$$\begin{aligned} -\mathcal{L}_{\mathrm{soft}} = & \Big(\sum_{i=1,1',2,3} M_i \lambda_i \lambda_i - A_s h_s S H_d H_u \\ & - A_u h_u U^c Q H_u - A_d h_d D^c Q H_d - A_e h_e E^c L H_d \\ & + \mathrm{H.c.} \Big) + m_{H_u}^2 |H_u|^2 + m_{H_d}^2 |H_d|^2 + m_s^2 |S|^2 \\ & + m_Q^2 \tilde{Q} \tilde{Q}^* + m_U^2 \tilde{U}^c \tilde{U}^{c*} + m_D^2 \tilde{D}^c \tilde{D}^{c*} \\ & + m_L^2 \tilde{L} \tilde{L}^* + m_E^2 \tilde{E}^c \tilde{E}^{c*} + \mathrm{H.c.}, \end{aligned} \tag{8}$$

where the sfermion mass-squareds $m^2_{Q,\ldots,E^c}$ and trilinear couplings $A_{u,\ldots,e}$ are 3×3 matrices in flavor space. All these soft masses will be taken here to be diagonal. In general, all gaugino masses, trilinear couplings, and flavor-violating entries of the sfermion mass-squared matrices are sources of CP violation [21]. In this work, however, for

simplicity and definiteness we will assume all of the parameters are real.

These soft supersymmetry-breaking parameters are subject to the renormalization group equations (RGEs) [22]. These equations should be used to evolve the soft parameters from high energy to low energy scales, which generally results in nonuniversal solutions around the weak scale. Instead, for simplicity, we will perform a general weak scale scan of the parameter space.

One of the attractive aspects of the U(1)′ model is that its Higgs sector is phenomenologically rich [23]. The Higgs sector of the model involves the singlet Higgs S and the electroweak doublets H_u and H_d all charged under the U(1)′ gauge group. The Higgs fields can be expanded around the vacuum state as follows:

$$H_u = \frac{1}{\sqrt{2}}\begin{pmatrix} \sqrt{2}H_u^+ \\ v_u + \phi_u + i\varphi_u \end{pmatrix},$$
$$H_d = \frac{1}{\sqrt{2}}\begin{pmatrix} v_d + \phi_d + i\varphi_d \\ \sqrt{2}H_d^- \end{pmatrix}, \tag{9}$$
$$S = \frac{1}{\sqrt{2}}(v_s + \phi_s + i\varphi_s),$$

where H_u^+ and H_d^- span the charged sector and the remaining ones span the neutral degrees of freedom, hence, $\phi_{u,d,s}$ are scalars and $\varphi_{u,d,s}$ are pseudoscalars. In the vacuum state

$$\frac{v_u}{\sqrt{2}} \equiv \langle H_u^0 \rangle, \qquad \frac{v_d}{\sqrt{2}} \equiv \langle H_d^0 \rangle, \qquad \frac{v_s}{\sqrt{2}} \equiv \langle S \rangle \tag{10}$$

and the $W^\pm$, Z, and Z' bosons all acquire masses. However, the neutral gauge bosons Z and Z' exhibit nontrivial mixing [3,16] as encoded in their mass-squared matrix:

$$(M_{Z-Z'})^2 = \begin{pmatrix} M_Z^2 & \delta_{Z-Z'}^2 \\ \delta_{Z-Z'}^2 & M_{Z'}^2 \end{pmatrix}. \tag{11}$$

Here

$$M_Z^2 = \frac{G^2}{4}[v_u^2 + v_d^2],$$
$$M_{Z'}^2 = g_Y'^2[Q_u^2 v_u^2 + Q_d^2 v_d^2 + Q_s^2 v_s^2], \tag{12}$$
$$\delta^2 = \frac{g_Y' G}{2}[Q_u v_u^2 - Q_d v_d^2],$$

and $G^2 = g_2^2 + g_1^2$. The two eigenvalues of the mass^2 matrix

$$m_{Z_1,Z_2}^2 = \frac{1}{2}[M_Z^2 + M_{Z'}^2 \mp \sqrt{(M_Z^2 - M_{Z'}^2)^2 + 4\delta_{Z-Z'}^4}] \tag{13}$$

give the masses of the physical massive vector bosons where m_{Z_1} must agree with the experimental bounds on the ordinary Z boson mass and m_{Z_2} weighs $\sim$1 TeV to be in accord with the experiments. The mixing angle following from diagonalization of $(M_{Z-Z'})^2$

$$\alpha_{Z-Z'} = \frac{1}{2}\arctan\left(\frac{2\delta_{Z-Z'}^2}{M_{Z'}^2 - M_Z^2}\right) \tag{14}$$

must be a few 10^{-3} for precision measurements at the LEP experiments to be respected. This puts another bound on the Z_2 boson mass. In particular, in generic E_6 models m_{Z_2} must weigh nearly a TeV or more according to the Tevatron measurements [17]. Besides this, the LHC can discover the additional Z boson if $m_{Z_2} \sim$ 4–5 TeV [24].

Related to the Higgs sector, the Higgs boson masses shift in proportion to particle-sparticle mass splitting under quantum corrections due to the soft breaking of supersymmetry. As in the MSSM, though all particles which couple to the Higgs fields S, H_u, and H_d contribute to the Higgs boson masses, the largest correction comes from the top and bottom quarks and their superpartners.

We will use the effective potential method [25] for computing the radiative corrections to Higgs potential. In the MSSM without corrections, the mass of the Higgs cannot be larger than M_Z. In U(1)′ models this is no longer true, but for a precise prediction radiative corrections are obligatory. The radiatively corrected potential reads as

$$V_{\text{total}}(H) = V_{\text{tree}}(H) + \Delta V(H), \tag{15}$$

where the tree level potential is composed of the F term, D term, and soft-breaking pieces

$$V_{\text{tree}} = V_F + V_D + V_{\text{soft}}, \tag{16}$$

with

$$V_F = |h_s|^2[|H_u \cdot H_d|^2 + |S|^2(|H_u|^2 + |H_d|^2)], \tag{17}$$

$$V_D = \frac{G^2}{8}(|H_u|^2 - |H_d|^2) + \frac{g_2^2}{2}(|H_u|^2|H_d|^2 - |H_u \cdot H_d|^2) + \frac{g_Y'^2}{2}\Delta^2, \tag{18}$$

$$V_{\text{soft}} = m_{H_u}^2|H_u|^2 + m_{H_d}^2|H_d|^2 + m_s^2|S|^2 + (h_s A_s S H_u \cdot H_d + \text{H.c.}). \tag{19}$$

In (18) we defined $\Delta = (Q_u|H_u|^2 + Q_d|H_d|^2 + Q_s|S|^2)$, for later convenience. The contributions of the quantum fluctuations in (15) read as

$$\Delta V = \frac{1}{64\pi^2}\,\text{Str}\left[\mathcal{M}^4\left(\ln\frac{\mathcal{M}^2}{\Lambda^2} - \frac{3}{2}\right)\right], \tag{20}$$

where $\text{Str} \equiv \sum_J (-1)^{2J}(2J+1)\text{Tr}$ is the usual supertrace which generates a factor of 6 for squarks and -12 for quarks. Λ is the renormalization scale and $\mathcal{M}$ is the field-dependent mass matrix of quarks and squarks (we assume $\Lambda = 1$ TeV). The dominant contribution comes from top and bottom sectors and the requisite top and bottom quark field-dependent masses read as

$$m_t^2(H) = h_t^2|H_u^0|^2, \qquad m_b^2(H) = h_b^2|H_d^0|^2. \tag{21}$$

Superpartners of fermions follow from the following general expression:

$$m_{\tilde{f}}^2 = \begin{pmatrix} M_{\tilde{f}LL}^2 & M_{\tilde{f}LR}^2 \\ M_{\tilde{f}RL}^2 & M_{\tilde{f}RR}^2 \end{pmatrix}, \tag{22}$$

where $f = t$ and b for top and bottom quarks. We also need $f = \mu$ terms for the muon. The entries of this mass-squared matrix read to be

$$M_{\tilde{f}LL}^2 = m_{L,\tilde{f}}^2 + m_f^2 + M_Z^2 \cos 2\beta (I_3^f - Q^f s_W^2) + Q_{f,L}\Delta, \tag{23}$$

$$M_{\tilde{f}RR}^2 = m_{R,\tilde{f}}^2 + m_f^2 + M_Z^2 \cos 2\beta (Q^f s_W^2) + Q_{f,R}\Delta, \tag{24}$$

$$M_{\tilde{f}LR}^2 = M_{\tilde{f}RL}^2 = m_f[A_f - h_s S\{\cot\beta, \tan\beta\}]. \tag{25}$$

In the above equations s_W stands for the sine of the Weinberg angle, I^f and Q^f stand for isospin and electric charge of the fermions but the $Q_{f,L}$ and $Q_{f,R}$ terms show the U(1)′ charges not to be mixed with the electric charges.

Insertion of the top and bottom mass matrices into (20) generates the full one-loop effective potential mass-squared matrix of the Higgs bosons

$$\mathcal{M}_{ij}^2 = \left(\frac{\partial^2}{\partial\Psi_i \partial\Psi_j} V_{\text{total}}\right)_0, \tag{26}$$

which follows from (15) with

$$\Psi_i \in \{\phi_u, \phi_d, \phi_s, \varphi_u, \varphi_d, \varphi_s\}. \tag{27}$$

The scalar components $\phi_{u,d,s}$ and pseudoscalar components $\varphi_{u,d,s}$ combine to generate the physical Higgs bosons. Two linearly independent combinations of $\varphi_{u,d,s}$ are the Goldstone bosons G_Z and $G_{Z'}$, which are eaten by the Z and Z' gauge bosons:

$$\begin{aligned} G_Z &= -\sin\beta\varphi_u + \cos\beta\varphi_d, \\ G_{Z'} &= \cos\beta\cos\alpha\varphi_u + \sin\beta\cos\alpha\varphi_d - \sin\alpha\varphi_s. \end{aligned} \tag{28}$$

The orthogonal combination

$$A = \cos\beta\sin\alpha\varphi_u + \sin\beta\sin\alpha\varphi_d + \cos\alpha\varphi_s \tag{29}$$

is the physical pseudoscalar Higgs boson and the mixing angle α is defined by

$$\cot\alpha \equiv \frac{v_u v_d}{v_s v}. \tag{30}$$

In addition to the pseudoscalar A, the spectrum contains scalar Higgs bosons h, H, and H'. Typically H' weighs close to m_{Z_2}. This extra scalar is the main difference from the MSSM spectrum in terms of the number of Higgs fields. In the numerical analysis we proposed $m_{Z_2} \leq 3$ TeV, but the LHC can diagnose properties of the additional Z boson up to $m_{Z_2} \sim 2$–2.5 TeV. In the following subsections we will present neutralino and chargino sectors and their contribution to the anomalous magnetic moment of the muon.

A. U(1)′ contribution to muon anomaly

As in the MSSM, chargino and neutralino sectors contribute to the anomalous magnetic moment of the muon. However, in the U(1)′ models μ entries of these two sectors are replaced by an effective term μ_{eff}. Besides this, due to the extra Z boson and the singlet field S, the number of neutralino states is increased. In the following parts we present related formulas for the anomalous magnetic moment of the muon, taken from Ref. [11]

1. Neutralino contribution

In the basis $(\tilde{B}, \tilde{W}_3, \tilde{H}_d^0, \tilde{H}_u^0, \tilde{S}, \tilde{Z}')$, the neutralino mass matrix can be written (in the simplest form [26]) as follows:

$$M_{\tilde{\chi}^0} = \begin{pmatrix} M_1 & 0 & -g_1 v_d/2 & g_1 v_u/2 & 0 & 0 \\ 0 & M_2 & g_2 v_d/2 & -g_2 v_u/2 & 0 & 0 \\ -g_1 v_d/2 & g_2 v_d/2 & 0 & -h_s v_s/\sqrt{2} & -h_s v_u/\sqrt{2} & g'_Y Q_d v_d \\ g_1 v_u/2 & -g_2 v_u/2 & -h_s v_s/\sqrt{2} & 0 & -h_s v_d/\sqrt{2} & g'_Y Q_u v_u \\ 0 & 0 & -h_s v_u/\sqrt{2} & -h_s v_d/\sqrt{2} & 0 & g'_Y Q_s v_s \\ 0 & 0 & g'_Y Q_d v_d & g'_Y Q_u v_u & g'_Y Q_s v_s & M_{1'} \end{pmatrix}. \tag{31}$$

The diagonalization of the mass matrix can be accomplished using a unitary matrix N,

$$N^T M_{\tilde{\chi}^0} N = \text{Diag}(M_{\tilde{\chi}_1^0}, \ldots, M_{\tilde{\chi}_6^0}). \tag{32}$$

The smuon mass-squared matrix can be extracted from (22), which can be diagonalized through the unitary matrix D as

$$D^\dagger M_{\tilde{\mu}}^2 D = \text{Diag}(M_{\tilde{\mu}_1}^2, M_{\tilde{\mu}_2}^2). \tag{33}$$

As can be inferred from Eqs. (23) and (24) we have additional D terms for scalar fermions including the smuon. With these definitions, the neutralino contribution to a_μ can be written as composed of two parts

$$a_\mu(\tilde{\chi}^0) = a_\mu^1(\tilde{\chi}^0) + a_\mu^2(\tilde{\chi}^0). \tag{34}$$

The first part reads

$$a_\mu^1(\tilde{\chi}^0) = \sum_{j=1}^{6}\sum_{k=1}^{2} \frac{m_\mu}{8\pi^2 M_{\tilde{\chi}_j^0}} \mathrm{Re}[L_{jk}R_{jk}^*] F_1\left(\frac{M_{\tilde{\mu}_k}^2}{M_{\tilde{\chi}_j^0}^2}\right) \quad (35)$$

and second part is

$$a_\mu^2(\tilde{\chi}^0) = \sum_{j=1}^{6}\sum_{k=1}^{2} \frac{m_\mu^2}{16\pi^2 M_{\tilde{\chi}_j^0}^2} (|L_{jk}|^2 + |R_{jk}|^2) F_2\left(\frac{M_{\tilde{\mu}_k}^2}{M_{\tilde{\chi}_j^0}^2}\right). \quad (36)$$

During the calculation, we need the following $\mu - \tilde{\mu} - \tilde{\chi}^0$ chiral couplings:

$$L_{jk} = \frac{1}{\sqrt{2}}(g_1 Y_{\mu_L} N_{1j}^* - g_2 N_{2j}^* + g_Y' Q_{\mu,L} N_{6j}^*) D_{1k} + \frac{\sqrt{2} m_\mu}{v_d} N_{3j}^* D_{2k} \quad (37)$$

and

$$R_{jk} = \frac{1}{\sqrt{2}}(g_1 Y_{\mu_R} N_{1j} + g_Y' Q_{\mu,R} N_{6j}) D_{2k} + \frac{\sqrt{2} m_\mu}{v_d} N_{3j} D_{1k}, \quad (38)$$

where $Y_{\mu_L} = -1$, $Y_{\mu_R} = 2$ are hypercharges and the loop integral functions are

$$F_1(x) = \frac{1}{2}\frac{1}{(x-1)^3}(1 - x^2 + 2x\ln x) \quad (39)$$

and

$$F_2(x) = \frac{1}{6}\frac{1}{(x-1)^4}(-x^3 + 6x^2 - 3x - 2 - 6x\ln x). \quad (40)$$

2. Chargino contribution

The chargino mass matrix is given by

$$M_{\tilde{\chi}^\pm} = \begin{pmatrix} M_2 & \sqrt{2} M_W \sin\beta \\ \sqrt{2} M_W \cos\beta & \mu_{\mathrm{eff}} \end{pmatrix}, \quad (41)$$

where $\mu_{\mathrm{eff}} = h_s v_s/\sqrt{2}$. This $M_{\tilde{\chi}^\pm}$ matrix can be diagonalized by two unitary matrices U and V as follows:

$$U^* M_{\tilde{\chi}^\pm} V^{-1} = \mathrm{Diag}(M_{\tilde{\chi}_1^\pm}, M_{\tilde{\chi}_2^\pm}). \quad (42)$$

Besides charginos, the sneutrino mass squared is needed:

$$M_{\tilde{\nu}_\mu} = m_{\tilde{L}}^2 + I_3^\nu M_Z^2 \cos 2\beta + Q_{\nu,L}\Delta. \quad (43)$$

As in the neutralino sector, the contribution of the chargino sector to the anomalous magnetic moment of the muon can be decomposed into two parts,

$$a_\mu(\tilde{\chi}^\pm) = a_\mu^1(\tilde{\chi}^\pm) + a_\mu^2(\tilde{\chi}^\pm). \quad (44)$$

The first part reads as

$$a_\mu^1(\tilde{\chi}^\pm) = \sum_{j=1}^{2}\sum_{k=1}^{1} \frac{m_\mu}{8\pi^2 M_{\tilde{\chi}_j^\pm}} \mathrm{Re}[L_{jk}R_{jk}^*] F_3\left(\frac{M_{\tilde{\nu}_\mu}^2}{M_{\tilde{\chi}_j^\pm}^2}\right) \quad (45)$$

and the second contribution is

$$a_\mu^2(\tilde{\chi}^\pm) = -\sum_{j=1}^{2}\sum_{k=1}^{1} \frac{m_\mu^2}{16\pi^2 M_{\tilde{\chi}_j^\pm}^2} (|L_{jk}|^2 + |R_{jk}|^2) F_4\left(\frac{M_{\tilde{\nu}_\mu}^2}{M_{\tilde{\chi}_j^\pm}^2}\right). \quad (46)$$

Here the chiral $\mu - \tilde{\nu}_\mu - \tilde{\chi}^\pm$ couplings are

$$L_{j1} = \frac{\sqrt{2} m_\mu}{v_d} U_{j2}^*, \qquad R_{j1} = -g_2 V_{j1}. \quad (47)$$

The loop integral functions are

$$F_3(x) = -\frac{1}{2}\frac{1}{(x-1)^3}(3x^2 - 4x + 1 - 2x^2\ln x) \quad (48)$$

and

$$F_4(x) = -\frac{1}{6}\frac{1}{(x-1)^4}(2x^3 + 3x^2 - 6x + 1 - 6x^2\ln x). \quad (49)$$

In the calculations we also implemented the leading-log contributions from two loop evaluation [27]

$$a_{\mu,2\,\mathrm{loop}}^{\mathrm{SUSY}} = a_{\mu,1\,\mathrm{loop}}^{\mathrm{SUSY}}\left(1 - \frac{4\alpha}{\pi}\ln\frac{M_{\mathrm{SUSY}}}{m_\mu}\right), \quad (50)$$

which yields a small suppression $\sim$7%. Based on this leading-log estimate we imposed a uniform 7% reduction in our numerical analysis.

It is appropriate to stress that we used the formulas given in [11] for the calculation of the anomalous magnetic moment of the muon, with a basic difference. In our definitions of the scalar muon $\tilde{\mu}$ and the scalar neutrino $\tilde{\nu}_\mu$, we explicitly stressed the D-term contributions on these particles. For the U(1)$'$ models considered here, these additional terms represented by Δ are also prevailing in the scalar fermions and hence introduce heavy model dependence, for each of the mentioned particles. On the other hand in more involved models, as in the secluded U(1)$'$ models [11], these contributions are not very important due to the presence of heavy Higgs singlets fields $S_{1,2,3}$.

III. NUMERICAL ANALYSIS

In this section we will present our numerical results. To begin with, during the analysis we respected the collider bounds on the sparticle masses, using Ref. [28], and imposed the following:

$$m_h > 114.4, \qquad m_{\tilde{t}_1} > 180, \qquad m_{\tilde{b}_1} > 240, \qquad m_{\tilde{\chi}_1^0} > 50, \qquad m_{\tilde{\chi}_1^\pm} > 170, \tag{51}$$

all in GeV. For the mass of the gauginos we assumed 50 GeV as the lower limit of M_1, M_2, and M_1'. We scanned M_1, M_2 up to 500 GeV; M_1' is scanned up to 2 TeV without imposing any unification relation. Additionally, for scalar quark masses we have considered mainly two cases: either squark mass eigenvalues can be as large as 2 TeV or, as a less fine-tuned alternative, they are smaller than 1 TeV. In our general scan, in addition to discarding $a_\mu < 0$ regions we also demanded the mass of the additional Z boson to be larger than 700 GeV and forced the mixing angle to obey $|\theta_{Z-Z'}| < 10^{-3}$. The trilinear couplings are scanned in the $|A_i| \leq 1$ TeV domain, where $i = t, b, \mu, s$ and soft masses are taken in the [0,1] TeV range. Notice that LL and RR entries of the scalar fermion mass^2 matrices are subject to the additional D terms of the U(1)$'$ models and hence not only zero but also negative values of the soft mass^2 terms can be considered in these entries. Related to model parameters, we demanded the Yukawa coupling h_s to be $\epsilon[0.1, 0.8]$ and confined $v_s \leq 10$ TeV to obtain large m_{Z_2} values as big as 3 TeV. In our scans, we also imposed a $\delta a_\mu > 0$ bound in addition to all of the mentioned constraints and created 80 000 data points for generic and E_6 models, separately.

In order to deal with the generic U(1)$'$ models we scanned the possible charges randomly. In doing this we allowed each of the charges Q_u, Q_d, Q_Q, and Q_L to vary randomly in the $[-1, 1]$ interval. Then Q_s, Q_U, Q_D, and Q_E values are obtained from the gauge anomaly conditions. For E_6 models the angle θ_{E_6}, which designates the charges, is scanned from 0 to π and phenomenologically acceptable charges coinciding with the mentioned boundaries are presented visually.

In a majority of the following figures we depicted the bounds coming from the muon anomaly constraint with straight gray lines where they represent 1σ and 2σ values belonging to $\delta a_\mu = (31.6 \pm 7.9) \times 10^{-10}$. In general, we will focus on 1σ ranges which results in tight constraints. But, as will be visible, when 2σ ranges are considered most of the stringent predictions vanish. Additionally, in all of the following figures our shading convention is such that black and gray dots exhibit the mass of the scalar fermions when they are lighter than 1 TeV and 2 TeV, respectively.

Our first figure is related to the allowed ranges of some of the generic U(1)$'$ charges against anomalous magnetic moment of the muon. To begin with, Fig. 1 serves to show that generic U(1)$'$ models possess an approximate symmetry for positive and negative U(1)$'$ charges. Moreover, some of the charges can be constrained to a certain extent. This approximate symmetry is true for any of the charges as can be seen from each panel of the figure. In generic U(1)$'$ models Q_Q and Q_D charges show certain tendencies (for instance $Q_Q \sim 0$ is more favored) but they are not constrained; in this respect Q_d behaves similarly. Nevertheless, larger $|Q_d|$ values are more probable than $Q_d \sim 0$, as can be seen from the related panels of Fig. 1. On the other hand, for the charges Q_u, Q_U, and Q_s there are illuminating constraints. As a concrete example, the U(1)$'$ charge of the Higgs singlet S should satisfy the interval

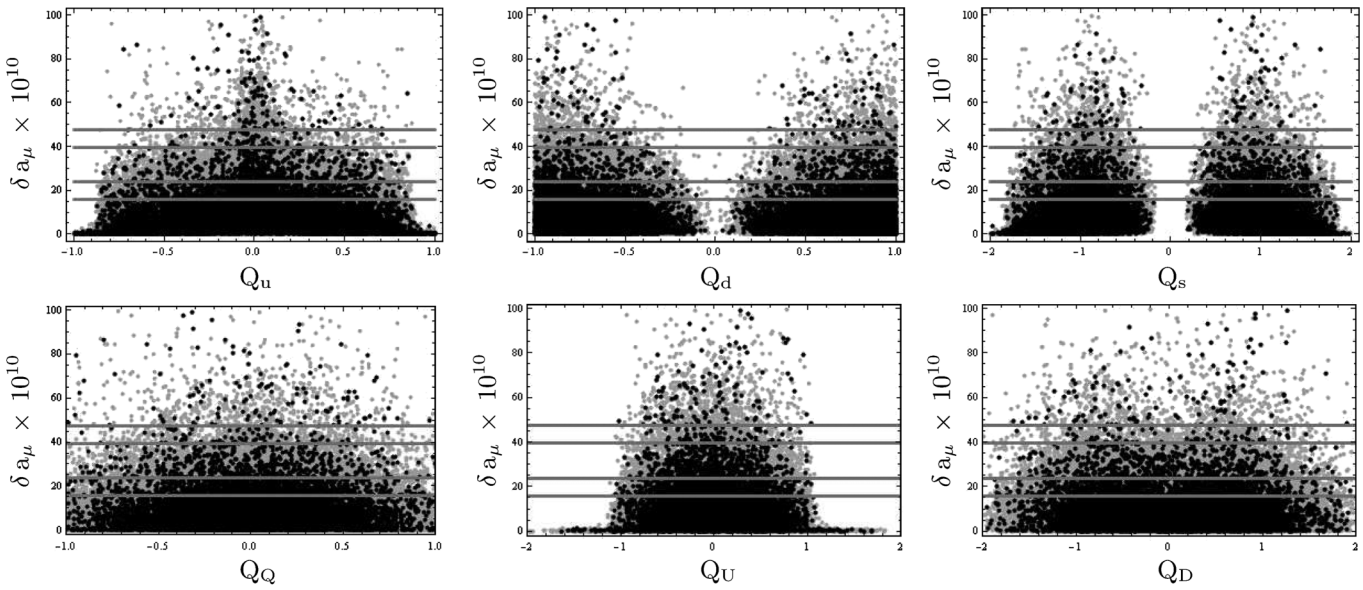

FIG. 1. The allowed ranges of the U(1)$'$ charges vs the anomalous magnetic moment of the muon in generic U(1)$'$ models. In this figure and the following ones, black dots depict $m_{\tilde{f}_2} < 1$ TeV and gray dots depict $m_{\tilde{f}_2} < 2$ TeV for $f = t, b$. The straight gray lines stand for 1σ and 2σ ranges.

$0.2 < |Q_s| < 1.8$ to respect the muon anomaly. This prediction does not change sensibly for 1 or 2σ ranges. This figure shows that certain portions of the generic $U(1)'$ models can be constrained by the anomalous magnetic moment of the muon. This is true at least for the charge of the singlet. Besides this, absolute values of the charges of the up Higgs field Q_u and the charge of the scalar up quarks Q_U should be around 1 even if we allowed the latter to be as large as 2. In fact, we should also present the $U(1)'$ charges of the leptons. But since the allowed parameter space will be further detailed with the bounds on the masses of the lightest Higgs and of the additional Z, toward the end of the analysis, it suffices to present some existential examples where some charges of the generic models can be constrained up to here.

For supersymmetric E_6 models we provide Fig. 2. This should be compared with Fig. 1, from which we observe that E_6 models are more sensitive to the imposition of the muon anomaly constraints than the generic $U(1)'$ models, as should be expected. Here, in supersymmetric E_6 models, instead of an approximate symmetry we observe two favorite regions satisfying the muon anomaly restrictions for any of the charges. Of course, this is true for 1σ bounds. These values can be translated back to the E_6 angle (θ_{E_6}) and this will be performed toward the end of the analysis with the additional constraints, as mentioned above.

Related to generic and E_6 models, it is important to compare their reactions when the restrictions from the muon anomaly are relaxed. As can be inferred from the Figs. 1 and 2, if the 2σ bound were applied instead of 1σ, then most of the constraints on E_6 model charges would vanish. On the other hand, the $U(1)'$ charges of the generic models are less sensitive to such a relaxation, as can be visualized from Fig. 1.

In Fig. 3 we present the mass of the lightest Higgs boson (m_h) against the vacuum ratio of up and down Higgs fields ($\tan\beta$) without additional constraints from the muon anomaly bounds, except $a_\mu > 0$. As can be seen from the left panel of Fig. 3, generic $U(1)'$ models can predict m_h as large as $m_h \sim 175$. Similarly, as can be seen from the right

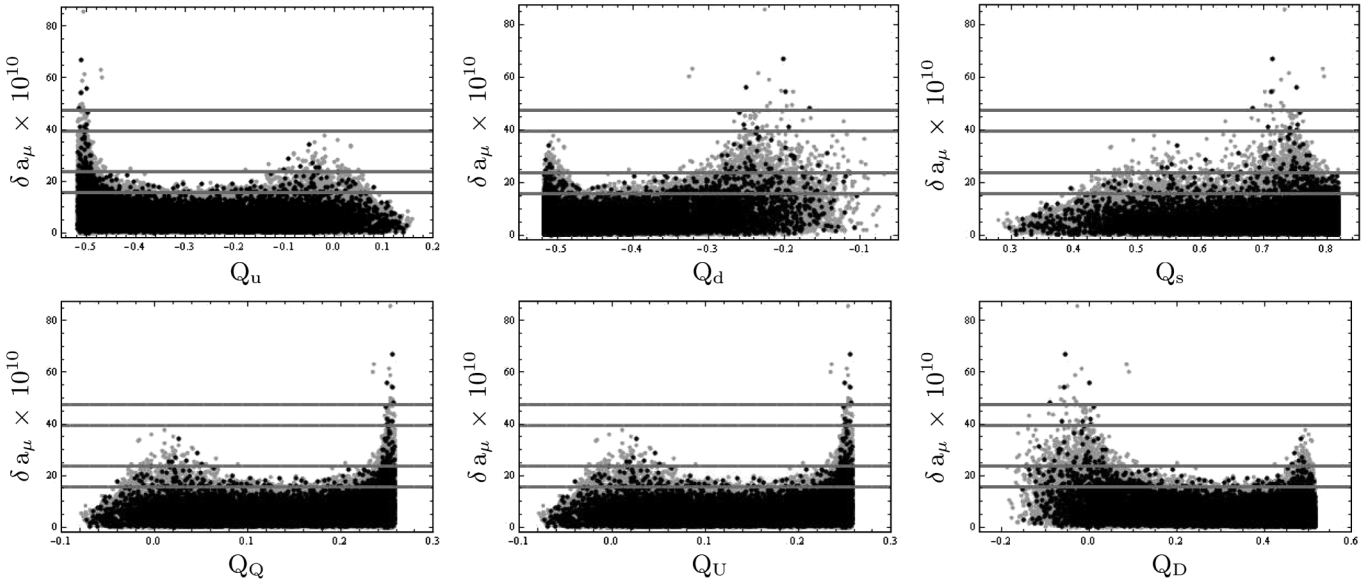

FIG. 2. As in Fig. 1 but for supersymmetric E_6 models.

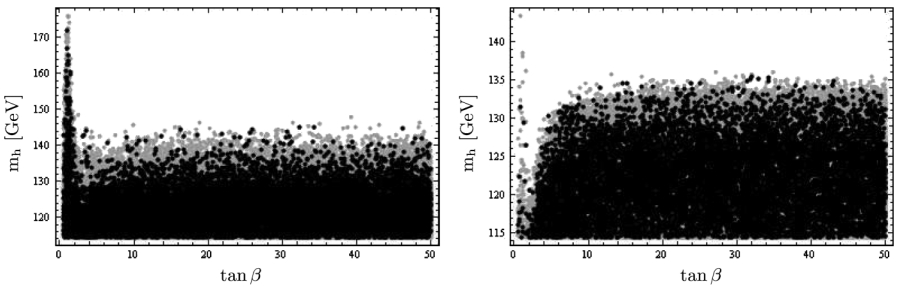

FIG. 3. The allowed ranges of $\tan\beta$ versus the mass of the lightest Higgs mass m_h in generic (left panel) and E_6 (right panel) models without the constraints from the anomalous magnetic moment of the muon.

panel of the same figure E_6 models can yield $m_h \sim 144$ GeV. As can be inferred from the comparison of gray and black dots, large values of m_h are easier to attain when the squark masses are large. It is clear from both of the panels in Fig. 3 that in U(1)′ models maximal value of the lightest Higgs mass m_h is possible only if $\tan\beta$ is very small, i.e., $\tan\beta \sim 1$. Indeed, around $\tan\beta \sim 1$ top Yukawa couplings are enhanced and this results in very large m_h predictions in comparison with the MSSM predictions. In regions where $\tan\beta > 5$ maximum value of the m_h prediction is almost constant up to $\tan\beta = 50$. On the other hand, it is known from the MSSM predictions that very small $\tan\beta$ values are ruled out due to the muon anomaly constraints. This point is important because these constraints can render large m_h predictions of the U(1)′ models, too.

So, in order to probe the allowed ranges of $\tan\beta$, in Fig. 4 we present $\tan\beta$ vs the anomalous magnetic moment of the muon. As can be seen from Fig. 4, $\tan\beta$ should be at least $\sim$10 in generic U(1)′ models and it should satisfy $\tan\beta > 15$ for E_6 models to be in accord with the anomalous magnetic moment of the muon boundaries. Of course, when 2σ ranges are considered, $\tan\beta$ can have smaller values. Here, dominant contributions come from chargino loops and since we considered $m_{\tilde{\chi}_1^\pm} > 170$ GeV, our boundaries demand $\tan\beta$ to be larger than the previous studies in which the chargino masses were satisfying $m_{\tilde{\chi}_1^\pm} > 104$ GeV. It should be noticed that the constraints on $\tan\beta$ values are more severe when the mass of the scalar fermions are confined to values smaller than 1 TeV, as can be seen from the black dots of the same figure. It is clear from Figs. 3 and 4 that in U(1)′ models very large values of m_h are not favored due to restrictions coming from the anomalous magnetic moment of the muon.

Another important observable within the U(1)′ models is the mass of the additional Z boson (m_{Z_2}). In order to show regions respecting the muon anomaly constraints we provide Fig. 5. As can be seen from the left panel of Fig. 5, generic U(1)′ models are not sensitive to the mass of the additional Z boson. On the other hand, as can be seen from the right panel of the same figure, E_6 models allow either $m_{Z_2} \sim 1$ TeV or $m_{Z_2} \sim 2$ TeV with a desert in between these two domains. While this m_{Z_2} excluding tendency is more strict for less fine-tuned scalar fermion masses ($m_{\tilde{t},\tilde{b}} < 1$ TeV) it is relaxed if $m_{\tilde{t},\tilde{b}} < 2$ TeV, as can be seen from the E_6 related panel of Fig. 5.

In Figs. 6 and 7 we present the allowed ranges of the charges for generic and E_6 models, respectively. In both of the figures all the mentioned constraints are respected and the resulting data show $m_{\tilde{t},\tilde{b}} < 2$ TeV and $m_{\tilde{t},\tilde{b}} < 1$ TeV domains of the scalar fermions in gray and in black dots, as in the previous figures. As can be seen from Fig. 6 when scalar fermions are light, constraints on the U(1)′ charges are more strict (black dots). This is also true for E_6 models, as can be seen from Fig. 7. It is easy to deduce from the first panel of Fig. 6 that, when the scalar fermions are light

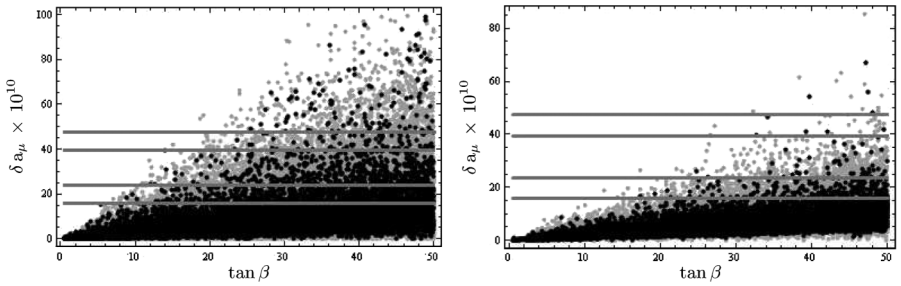

FIG. 4. The evolution of $\tan\beta$ against the anomalous magnetic moment of the muon in generic (left panel) and E_6 (right panel) models.

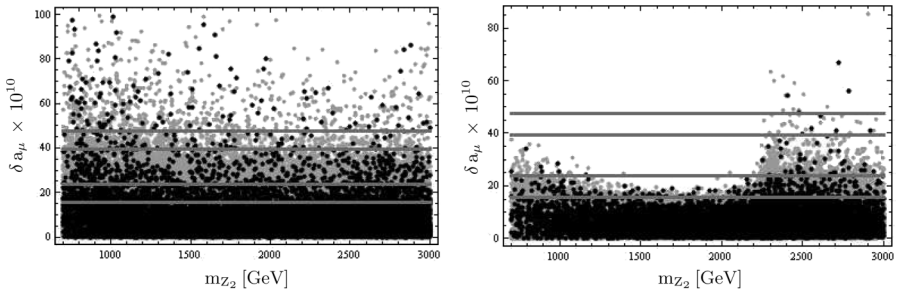

FIG. 5. An illustration of the allowed ranges of the mass of the additional Z boson m_{Z_2} versus the anomalous magnetic moment of the muon in generic (left panel) and E_6 (right panel) models.

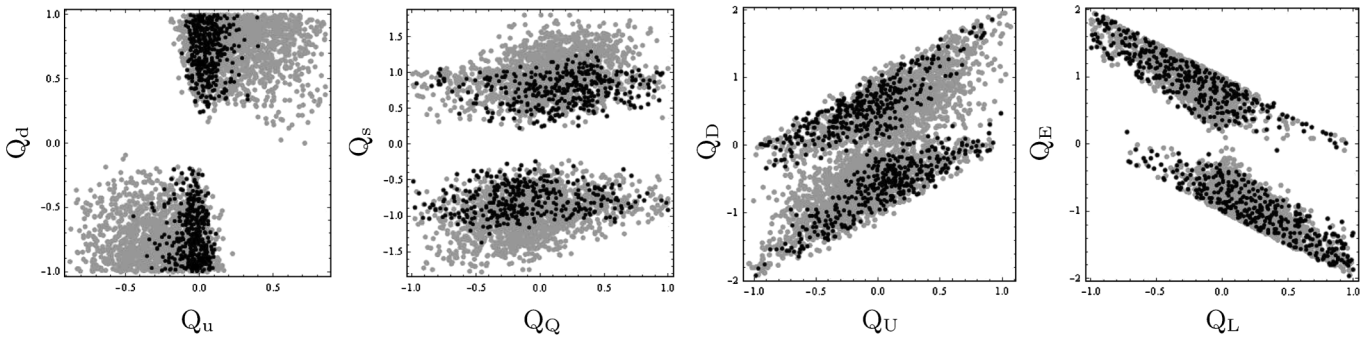

FIG. 6. The allowed ranges of the U(1)′ charges against each other in generic U(1)′ models respecting all the mentioned constraints. In this figure and the following ones, the 1σ range is considered for the anomalous magnetic moment of muon.

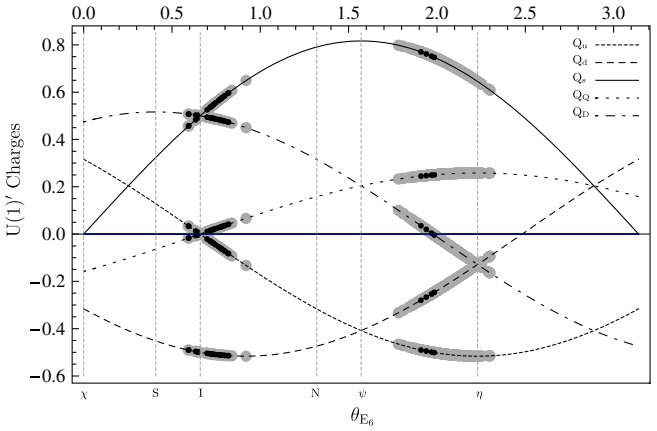

FIG. 7 (color online). The allowed ranges of the U(1)′ charges versus the E_6 angle.

(black dots representing $m_{\tilde{l},\tilde{b}} < 1$ TeV) the U(1)′ charge of the up Higgs field prefers $Q_u \sim 0$ and it can be relaxed up to $|Q_u| < 0.5$, but the U(1)′ charge of the down Higgs field should, at least, satisfy $|Q_d| > 0.2$ in order to be consistent with the anomalous magnetic moment of the muon. Similar conclusions can be extracted from the other panels of the figures—instead, we present them in tabulated form in Table II.

For supersymmetric E_6 models the situation is simpler because here any of the charges can be expressed by using the angle of the E_6 models. As can be seen from Fig. 7, two values $\theta_{E_6} \sim 0.7$ and $\theta_{E_6} \sim 2$ are favored for E_6 models, which correspond to I and η models, respectively. Actually, the η model is marginally consistent with the muon anomaly conditions but the model I is current for both of the cases: $m_{\tilde{l},\tilde{b}} < 1$ TeV and 2 TeV cases as can be seen from the black and gray dots of the figure. For a tabulated form of the allowed ranges of the fields we refer to Table II.

Our last figure is devoted to the mass of the lightest Higgs boson m_h versus the mass of the additional Z boson m_{Z_2}. As can be seen from the left panel of Fig. 8, in generic U(1)′ models the upper limit of m_h increases as m_{Z_2} gets heavier. The maximum value of m_h consistent with all the mentioned constraints turns out as $m_h^{\max} \sim 140$ GeV. This upper limit is sensitive to the mass of additional Z boson for which we considered $m_{z_2} \leq 3$ TeV and it is also dependent on the mass of the scalar fermions as should be deduced from the gray dots. However, if the masses of the scalar quarks are less than 1 TeV then the mass of the lightest Higgs should be smaller than ~128 GeV and the mass of the additional Z should be smaller than ~2.3 TeV, as can be seen from the black dots.

The situation is similar but more strict for E_6 models, as can be seen from the right panel of Fig. 8. Supersymmetric E_6 models predict that $m_h^{\max} \sim 135$ GeV if squarks are heavy (gray dots), it cannot be larger than ~125 GeV if squarks are within the TeV range (black dots). Additionally, according to E_6 models, at least within the

TABLE II. The allowed ranges of the absolute maximum (minimum) values of the U(1)′ charges for different scalar fermion masses in generic and E_6 models with 1σ range for the anomalous magnetic moment of the muon. In E_6 models two favored regions can be expressed by using the angle θ_{E_6}, which are, approximately, $\theta_{E_6} = 0.75 \pm 0.2$ and $\theta_{E_6} = 2.05 \pm 0.3$, as can be seen from Fig. 7.

	$\lvert Q_u\rvert$	$\lvert Q_d\rvert$	$\lvert Q_s\rvert$	$\lvert Q_Q\rvert$	$\lvert Q_U\rvert$	$\lvert Q_D\rvert$	$\lvert Q_L\rvert$	$\lvert Q_E\rvert$
Generic and $m_{\tilde{f}} \leq 1$ TeV	0.45(0)	1(0.19)	1.37(0.23)	1(0)	0.99(0)	1.92(0)	0.99(0)	1.96(0)
Generic and $m_{\tilde{f}} \leq 2$ TeV	0.88(0)	1(0)	1.81(0.21)	1(0)	1.07(0)	1.96(0)	1(0)	1.96(0)
E_6 and $m_{\tilde{f}} \leq 1$ TeV	0.50(0)	0.51(0.25)	0.77(0.46)	0.25(0)	0.25(0)	0.51(0)	0.51(0)	0.25(0)
E_6 and $m_{\tilde{f}} \leq 2$ TeV	0.52(0)	0.52(0.09)	0.79(0.46)	0.26(0)	0.26(0)	0.51(0)	0.51(0)	0.26(0)

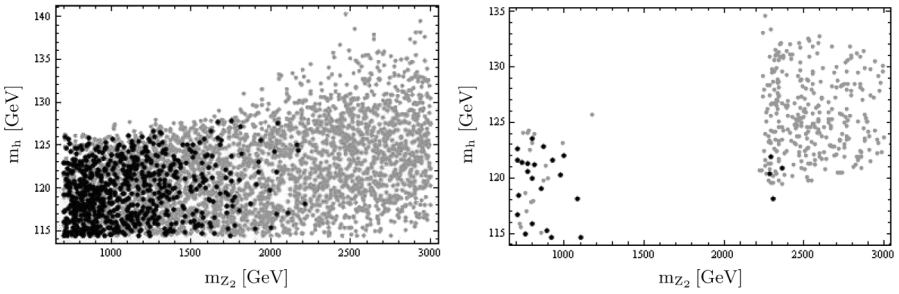

FIG. 8. The allowed ranges of mass of the lightest Higgs boson (m_h) against second neutral Z mass m_{Z_2}. Here we applied $m_{\tilde{f}} < 1$ TeV (black dots) and $m_{\tilde{f}} < 2$ TeV (gray dots) bounds as explained in the previous figures.

assumptions we made, E_6 models predict m_{Z_2} around 1 TeV or mass of the additional Z boson should be larger than ~2.2 TeV to satisfy the boundaries from the anomalous magnetic moment of the muon.

IV. CONCLUSIONS

In this work we used a 1σ range of the observed anomaly in the magnetic moment measurements of the muon and applied this information to find constraints on the generic and E_6-based U(1)′ models. We observed that certain portions of the parameter space of the U(1)′ models can satisfy this anomaly. We extracted bounds on the free charges of the generic U(1)′ models and of the E_6 models.

From the imposition of theoretical considerations and of experimental bounds we have obtained predictions for the mass of the lightest Higgs boson (m_h) and of the additional Z boson m_{Z_2} in generic and E_6 models. We observed that U(1)′ models allow m_{Z_2} to be as large as 3 TeV if the scalar fermions are bounded from above by $m_{\tilde{f}} \leq 2$ TeV. However smaller sfermion masses ($m_{\tilde{f}} \leq 1$ TeV) also squeeze m_{Z_2} to smaller values and it can be around ~2 TeV, at most.

In generic U(1)′ models, if scalar quarks are allowed to be heavy (i.e. $m_{\tilde{f}} < 2$ TeV) then the mass of the lightest Higgs could be as large as 145 GeV. However if the scalar fermions are lying within the 1 TeV range then m_h cannot be larger than 128 GeV, according to generic U(1)′ models. For E_6 models, heavy sfermions allow m_h to be as large as ~135 GeV, but if the sfermions are light then m_h cannot exceed 125 GeV, respecting the anomalous magnetic moment of the muon. These observations are true for the 1σ range of the observed anomaly in the magnetic moment measurements of the muon. It is visible from the figures given in the previous section that when a 2σ range or more conservative intervals are considered, most of the bounds obtained in this work would shift to some extent. For instance, due to smaller $\tan\beta$ prediction m_h can gain a few additional GeVs. On the other hand, while generic U(1)′ charges are not very sensitive to 1 or 2σ ranges, stringent bounds on the E_6 models relax significantly.

The bounded parameter space and predictions obtained in accord with the anomalous magnetic moment of the muon anomaly involve important projections for future measurements [29], especially of Higgs mass which will be observed at the LHC.

ACKNOWLEDGMENTS

We thank Paul Langacker for helpful discussions. The work of Z. K. was partially supported by the Scientific and Technical Research Council of Turkey.

[1] S. P. Martin, arXiv:hep-ph/9709356.
[2] J. E. Kim and H. P. Nilles, Phys. Lett. **138B**, 150 (1984); G. F. Giudice and A. Masiero, Phys. Lett. B **206**, 480 (1988).
[3] M. Cvetic, D. A. Demir, J. R. Espinosa, L. L.Everett, and P. Langacker, Phys. Rev. D **56**, 2861 (1997); **58**, 119905 (E) (1998); P. Langacker and J. Wang, Phys. Rev. D **58**, 115010 (1998).
[4] G. W. Bennett *et al.* (Muon G-2 Collaboration), Phys. Rev. D **73**, 072003 (2006).
[5] M. Passera, W. J.Marciano, and A. Sirlin, arXiv:1001.4528.
[6] M. Passera, J. Phys. G **31**, R75 (2005).
[7] M. Davier *et al.*, Eur. Phys. J. C **66**, 127 (2010).
[8] M. Passera, W. J. Marciano, and A. Sirlin, AIP Conf. Proc. **1078**, 378 (2009).
[9] S. P. Martin and J. D. Wells, Phys. Rev. D **64**, 035003 (2001).
[10] F. Domingo and U. Ellwanger, J. High Energy Phys. 07 (2008) 079.

[11] V. Barger, C. Kao, P. Langacker, and H. S. Lee, Phys. Lett. B **614**, 67 (2005).
[12] D. A. Demir, L. L. Everett, M. Frank, L. Selbuz, and I. Turan, Phys. Rev. D **81**, 035019 (2010).
[13] S. F. King, S. Moretti, and R. Nevzorov, Phys. Lett. B **634**, 278 (2006); Phys. Rev. D **73**, 035009 (2006); V. Barger, P. Langacker, H. S. Lee, and G. Shaughnessy, Phys. Rev. D **73**, 115010 (2006).
[14] D. A. Demir, L. Solmaz, and S. Solmaz, Phys. Rev. D **73**, 016001 (2006).
[15] H. Sert, E. Cincioğlu, D. A.Demir, and L. Solmaz, arXiv:1005.1674.
[16] P. Langacker, Rev. Mod. Phys. **81**, 1199 (2009).
[17] J. Erler, P. Langacker, S. Munir, and E. R. Pena, J. High Energy Phys. 08 (2009) 017.
[18] D. A. Demir, G. L. Kane, and T. T. Wang, Phys. Rev. D **72**, 015012 (2005); A. Hayreter, Phys. Lett. B **649**, 191 (2007).
[19] D. Suematsu, T. Toma, and T. Yoshida, arXiv:0910.3086.
[20] J. Erler, Nucl. Phys. **B586**, 73 (2000).
[21] D. A. Demir and L. L. Everett, Phys. Rev. D **69**, 015008 (2004).
[22] D. A. Demir, J. High Energy Phys. 11 (2005) 003; P. Langacker, G. Paz, L. T. Wang, and I. Yavin, Phys. Rev. D **77**, 085033 (2008).
[23] V. Barger, P. Langacker, H. S. Lee, and G. Shaughnessy, Phys. Rev. D **73**, 115010 (2006).
[24] P. Langacker, AIP Conf. Proc. **1200**, 55 (2010).
[25] S. R. Coleman and E. J. Weinberg, Phys. Rev. D **7**, 1888 (1973).
[26] S. Y. Choi, H. E. Haber, J. Kalinowski, and P. M. Zerwas, Nucl. Phys. **B778**, 85 (2007).
[27] G. Degrassi and G. F. Giudice, Phys. Rev. D **58**, 053007 (1998).
[28] C. Amsler *et al.* (Particle Data Group), Phys. Lett. B **667**, 1 (2008).
[29] V. Barger, P. Langacker, M. McCaskey, M. J. Ramsey-Musolf, and G. Shaughnessy, Phys. Rev. D **77**, 035005 (2008).